

Journal of Alloys and Compounds 401 (2005) 64-68



www.elsevier.com/locate/jallcom

# Revealing the structural disturbances in Czochralski silicon by high temperature—pressure treatment

J. Bak-Misiuk<sup>a,\*</sup>, A. Shalimov<sup>a</sup>, A. Misiuk<sup>b</sup>, J. Härtwig<sup>c</sup>, J. Trela<sup>a</sup>

<sup>a</sup> Institute of Physics, Polish Academy of Sciences, PAS, Al. Lotnikow 32/46, 02-668 Warsaw, Poland
<sup>b</sup> Institute of Electron Technology, Al. Lotnikow 46, 02-668 Warsaw, Poland
<sup>c</sup> European Synchrotron Radiation Facility, F-38043 Grenoble, Cedex 9, France

Received 19 August 2004; received in revised form 31 January 2005; accepted 31 January 2005 Available online 7 July 2005

#### **Abstract**

High-resolution X-ray diffraction and topographic methods were used to characterize the structural defects in single crystalline Czochralskigrown silicon (Cz-Si) with various oxygen concentrations. Annealing under hydrostatic pressure (HP) was applied for revealing the defects existing in Cz-Si wafers. The high pressure—high temperature treatment of as-grown Cz-Si at 1127 °C under 1.1 GPa resulted in enhanced oxygen precipitation, mostly at the initially existing structural disturbances, while annealing under 10<sup>7</sup> Pa did not affect the defect structure in the sample. The visibility of defects after the treatment under high pressure can be related to HP-induced strain at the boundary between the defect and the Si matrix, to increased defect dimensions due to HP-stimulated oxygen precipitation and to decreased concentration of defects. Precipitation of oxygen on small structural inhomogeneities and agglomeration of small defects assist in revealing the structural disturbances pre-existing in Cz-Si.

© 2005 Elsevier B.V. All rights reserved.

Keywords: Silicon; Defect structure; High pressure treatment; Semiconductors; X-ray diffraction; Point defects

#### 1. Introduction

Single crystalline silicon grown by Czochralski method (Cz-Si) contains oxygen in interstitial positions (O<sub>i</sub>). Oxygen interstitials are clustering and precipitating at annealing, mostly on the initially present structural inhomogeneities. Oxygen precipitation occurs during prolonged annealing at  $900-1000\,^{\circ}\text{C}$  while short-time one-step processing at  $\geq 1100\,^{\circ}\text{C}$  exerts almost no effect in this respect. Single crystalline Cz-Si is typically considered as free of extended defects; no dislocations are usually revealed by X-ray (synchrotron) topography. It is known, however, that treatment under enhanced hydrostatic pressure (HP) promotes oxygen precipitation on structural disturbances even at  $\sim 1130\,^{\circ}\text{C}$  if done for a prolonged time (e.g. for 5 h [1]).

The structural defects can cause extended strain fields in single crystals, therefore they are detected by X-ray topography or by X-ray diffuse scattering methods; 'small' defects with submicron sizes, which are not detectable on topographs, result in increase of diffuse scattering intensity. It should be noted, that X-ray methods are much more sensitive to the strain fields that surround the precipitates than to the defects itself. The notions of 'small' and 'large' defects used below concern the strain field size.

The purpose of the present work is to reveal oxygen precipitation sites and in this way also initially existing disturbances in Cz-Si by the short-time treatment at 1127 °C under HP followed by X-ray topography and diffuse scattering examination.

### 2. Experimental

The 0.6 mm thick (001)-oriented Cz-Si samples with various initial O<sub>i</sub> concentrations,  $c_0$  (8 × 10<sup>17</sup> cm<sup>-3</sup> for the

<sup>\*</sup> Corresponding author. Tel.: +48 22 843 6034; fax: +48 22 843 0926. *E-mail address:* bakmi@ifpan.edu.pl (J. Bak-Misiuk).

samples A and  $11 \times 10^{17} \, \mathrm{cm^{-3}}$  for samples B) cut from commercially available Si wafers, were used in the study. Additionally, samples C prepared by pre-annealing of the samples B at 450 °C under  $10^5$  Pa for 20 h were investigated. Such pre-annealing results in creation of oxygen nanoclusters exhibiting thermal donor activity and in a decrease of  $c_0$  ( $c_0 = 9 \times 10^{17} \, \mathrm{cm^{-3}}$  for the C).

Next, the samples were treated for 2 h at  $1127\,^{\circ}\text{C}$  under  $10^7\,\text{Pa}$  or  $1.1\,\text{GPa}$  [2]. Their defect structure was then determined by X-ray synchrotron topography (performed at the ID 19 synchrotron beamline of ESRF) as well as from the 004 rocking curve and reciprocal space mapping using the high-resolution X-ray MRD Philips diffractometer in the double and triple axis configurations. The lattice parameters of all samples were measured by the method described by Fewster and Andrew in Ref. [3]. The concentration of oxygen interstitials,  $c_0$ , was determined by Fourier Transform Infrared Spectroscopy, FTIR.

#### 3. Theoretical considerations

The characteristics of small defects, not detected by X-ray topography, can be estimated from diffuse scattering examination of the rocking curve in the Huang region (e.g. [4–6]). The X-ray scattering arises from the long-range displacement fields associated with various defects. The defect sizes for samples B and C were estimated from the dependence of the diffuse scattering intensity  $(I_S)$  on the deviation from the Bragg angle at the incidence angles corresponding to the transition from the Huang to Stokes-Wilson region [4,5] and by the method described by Patel [5], from the linear plot  $I_S(q_0)$ versus  $\ln q_0$  ( $q_0$  means the minimum value of deviation of the scattering vector, q, from the reciprocal lattice vector). For sample A, where the transition from Huang to Stokes-Wilson scattering was not detected, the dimension of defects was estimated using only the latter method. The defect concentrations for the B and C samples were calculated from the difference between the Huang and thermal diffuse scattering intensities measured for the same q value [5] (with exception of samples A where this difference did not exist). The log-log plot of the symmetrical part I of the diffuse scattering intensities, as a function of the deviation from the Bragg angle, consists of three parts related to the Huang, Wilson-Stokes and thermal scattering [6]. The intensities of thermal scattering  $(I_T)$  and Huang scattering  $(I_H)$ , are described by the same law  $(I \sim q^{-2})$ , but for smaller values of q [5]. The ratio of Huang diffuse scattering intensity to the thermal diffuse scattering intensity depends on the concentration and dimension of oxygen clusters [6], according to the formula:

$$\frac{I_{\rm H}(q_{\rm H})|Iq_{\rm H}|^2}{I_{\rm T}(q_{\rm T})|Iq_{\rm T}|^2} \approx \frac{n_{\rm d}\Delta V^2}{K} \tag{1}$$

where  $n_d$  is the defect concentration,  $K = k_B T/E$ ,  $k_B$ , the Boltzmann constant, T, the temperature of the sample, E, the Young

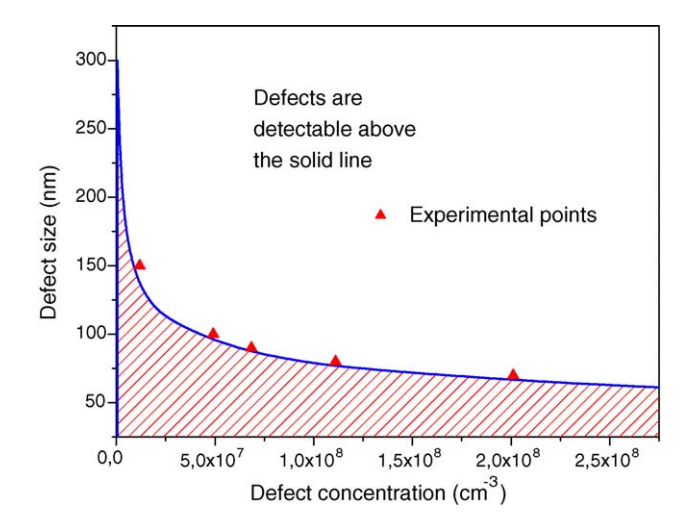


Fig. 1. Calculated plot of defect sizes vs. their concentration. The range of sizes and defect concentrations which cannot be estimated from diffuse scattering is shown as a shadowed area. Triangles correspond to data for B and C samples treated under 10<sup>7</sup> Pa and 1.1 GPa.

modulus,  $\Delta V$ , the volume change which can be obtained from the calculated defect size,  $q_{\rm H}$ , the value of q in any point of the Huang scattering region, and  $I_{\rm H}(q_{\rm H})$  the measured intensity in that point;  $q_T$  and  $I_T(q_T)$ , are the analogous values in the thermal scattering region.

From the size of oxygen clusters their concentration can be calculated, for the case of  $I_{\rm H}/I_{\rm T} > 1$ , using formula (1). The region of defect sizes and of their concentrations within which defect characteristics cannot be calculated from the diffuse scattering data ( $I_{\rm H}/I_{\rm T} < 1$ ) is presented in Fig. 1.

## 4. Results and discussion

Due to small dimensions of the defects and their high concentration, no contrast coming from oxygen precipitates or dislocations was found for all samples treated under 10<sup>7</sup> Pa (Fig. 2), while the treatment under 1.1 GPa resulted in creation of a high concentration of small precipitates (Fig. 2), best detected for the sample with the smallest oxygen concentration. For the higher defect concentrations (B samples), the contrast from defects is much less resolved. Pre-annealing of B samples to produce C samples results in a creation of a high concentration of small defects and, consequently, due to numerous nucleation centers, the precipitation contrast is less visible on topographs. The density of defects after the treatment, calculated from topographical images, was found to be of about  $5 \times 10^2 \,\mathrm{cm}^{-2}$  for samples A;  $1 \times 10^3 \,\mathrm{cm}^{-2}$ for sample B and  $6 \times 10^2 \, \text{cm}^{-2}$  for samples C. Low defect density observed on the topographs and their lower contrast proved the high concentration of small defects, not detectable on the topographs but influencing the diffuse scattering.

For samples A, due to small defect concentration, diffuse scattering observed on the reciprocal space maps as an enlargement of central peak is practically independent on applied pressure (Fig. 3). For samples B and C with higher

# Download English Version:

# https://daneshyari.com/en/article/9803379

Download Persian Version:

https://daneshyari.com/article/9803379

Daneshyari.com